14th International Symposium on Turbulence and Shear Flow Phenomena (TSFP14)
Heidelberg, Germany, July 28–31, 2026

RESTRICTED NONLINEAR BOUNDARY LAYER TRANSITION

Benjamin A. Minnick
Maneuvering and Control Division
Naval Surface Warfare Center
9500 MacArthur Blvd.
West Bethesda, MD, 20817, USA
benjamin.a.minnick.civ@us.navy.mil

Alexandra C. Risha
Dept. of Mechanical Eng.
Johns Hopkins University
3400 N. Charles St.
Baltimore, MD, 21218, USA
arisha1@jh.edu

Dennice F. Gayme
Dept. of Mechanical Eng.
Johns Hopkins University
3400 N. Charles St.
Baltimore, MD, 21218, USA
dennice@jhu.edu

ABSTRACT

This study employs the restricted nonlinear (RNL) model to interrogate the temporal evolution of flow structures during K-type transition. The RNL model retains cross-stream nonlinearity in its streamwise-averaged mean dynamics, but obtains order reduction by omitting nonlinear interactions between streamwise-varying perturbations that do not contribute to the mean. Further order reduction is achieved by limiting the number of streamwise-varying Fourier modes supporting the perturbation dynamics. This reduced system permits tractable study of perturbation growth known to be critical in laminar-turbulent transition but difficult to interrogate with direct numerical simulation (DNS). Results demonstrate RNL dynamics supported by a single streamwise-varying Fourier mode transition to turbulence later than DNS without Tollmien-Schlichting (TS) wave saturation, however, salient transitional flow features are retained including roll-up of the shear-layer. These findings demonstrate the utility of the RNL model to study transition and motivate its use as the basis for developing a minimal model for transition. We explore spanwise-mode truncation in the RNL model, as well as minor augmentation of its streamwise-varying dynamics to improve the prediction of transition location. Spanwise-mode truncation shows little to no effect on prediction accuracy, but the addition of a single streamwise-varying mode that is permitted to interact with others is shown to greatly improve it.

MOTIVATION

Maneuvering and control predictions for naval vessels and aircraft rely on accurate determination of transition location within the boundary layer surrounding the vehicle. Reynolds-Averaged Navier-Stokes (RANS) simulations are typically the engineering tool of choice to study flow over these vehicles, informing design and control algorithms. RANS has been used in the study of indicator functions for turbo-machinery blades (Menter *et al.*, 2022), development of a transition model for flow over a prolate spheroid (Aram *et al.*, 2022), and application of uncertainty quantification for airfoil flow (Jung & Baeder, 2023) among others. RANS tools benefit from relatively low computational expense but accurate prediction of the transition location is sensitive to the closure method used.

The difficulty in modeling transition using the RANS perspective has encouraged researchers to interrogate the transition flow process directly. For example, embedding direct numerical simulations (DNS) into the RANS computation to obtain a more reliable prediction in transition location (Y. Mori & Obayashi, 2024). DNS has also been used in canonical studies, proving to be a valuable tool for identifying transitional flow structures (Zaki, 2013; Marxen & Zaki, 2019; Lee & Jiang, 2026), otherwise masked in RANS models. So-called Λ-vortices are particularly prevalent in studies of natural transition and responsible for the generation of a shear layer that drives the flow to transition to turbulence. These transitional flow structures organize into streaks and rolls involved with sustaining the turbulence (Lee & Jiang, 2026).

The high computational expense of DNS has motivated the use of lower cost methods that maintain a desired level of fidelity in transitional flow studies. Large eddy simulations (LES) with sub-grid scale models employing de-convolution have proven successful in reproducing transitional flow structures (Schlatter *et al.*, 2004, 2006). LES employing nonlinear parabolized stability equations as inflow have similarly been shown to predict the point of transition (Lozano-Durán A. & Moin, 2018) at lower computational costs. Another alternative includes the use of machine-learning classifiers to aid the LES wall-model for accurate laminar/turbulent region predictions (Narasimhan *et al.*, 2021).

This work employs a reduced-order model capable of resolving key structural flow features in wall-bounded turbulence. Inspired by streamwise coherent structures, the restricted nonlinear (RNL) model has been described as a minimal model for the self-sustaining process (Thomas *et al.*, 2015). The RNL model decomposes the flow into streamwise-averaged mean (large-scale) and streamwise-varying perturbation (small-scale) components where nonlinear interactions are restricted to those that contribute to the mean. Order reduction is achieved through this restriction and truncation of the streamwise-varying dynamics, while a full range of the cross-stream nonlinear modal interactions is maintained. This approach has been shown to accurately predict low-order statistics (Gayme & Minnick, 2019) and been applied to develop control for drag reduction (Han *et al.*, 2024).

Recently, the RNL dynamics of developing boundary layers over moving walls have been studied (Risha *et al.*, 2026; Minnick & Gayme, 2024). These RNL simulations reproduce known trends in low-order statistics for boundary layers exposed to favorable and adverse conditions. Furthermore, interrogation of the RNL mean and perturbation components in these studies have highlighted the role large and small streamwise-scales play in flow development. This tractability makes the RNL model an appealing dynamical system to study transition to isolate and interrogate scale interactions.

This paper is organized as follows. In the technical approach, we first review the initial and boundary conditions used to produce K-type transition. The RNL model is then

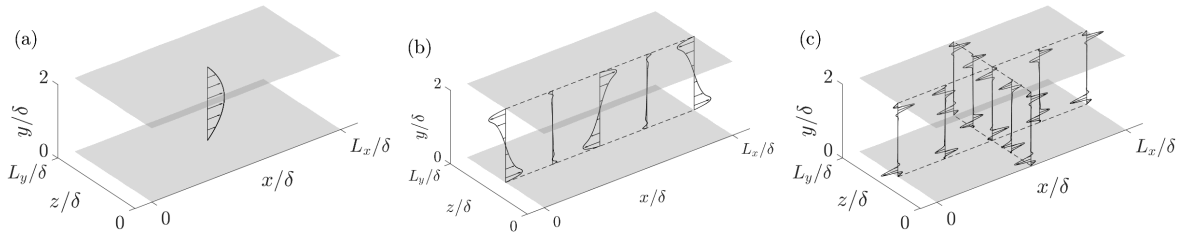

Figure 1. Initial condition components including: (a) laminar base flow, (b) 2D TS wave, and (c) three-dimensional oblique wave. Only the streamwise velocity component is shown.

introduced and formulated within the context of studying transition in a temporally developing boundary layer. The results section details the RNL transition process and the evolution and interaction of the streamwise-mean and streamwise-varying perturbation components. Time histories of the wall-stress and energy of Fourier modes are compared to DNS to identify the role of the streamwise-varying interactions absent in the RNL dynamics. We then further analyze this role by augmenting the RNL model with additional streamwise-varying interactions, which leads to improved prediction of the transition time. The results section ends with a discussion of truncating spanwise modes supporting the RNL dynamics. This paper then concludes with a summary of findings and possible directions for future work.

TECHNICAL APPROACH

We consider a flow configuration similar to Schlatter *et al.* (2006), that is prone to temporal K-type transition (Klebanoff *et al.*, 1962). The initial condition is a superposition of a quadratic laminar base profile, a two-dimensional (2D) Tollmien-Schlichting (TS) wave, and three-dimensional (3D) oblique wave, leading to

$$\mathbf{u}_\mathrm{T}(\mathbf{x},t=0) = u_B(y)\mathbf{e}_x + \varepsilon_{2D}\mathbf{u}_{2D}(y)e^{i\alpha x} + \frac{1}{2}\varepsilon_{3D}e^{i\alpha x}\left[\mathbf{u}^+_{3D}(y)e^{i\beta z} + \mathbf{u}^-_{3D}(y)e^{-i\beta z}\right]. \quad (1)$$

We take $\mathbf{x} = (x,y,z)$ to respectively denote the streamwise, wall-normal, and spanwise directions, and t to denote the temporal coordinate. The amplitudes of the initial perturbations are $\varepsilon_{2D} = 0.03\mathscr{U}$ and $\varepsilon_{3D} = 0.001\mathscr{U}$, where $\mathscr{U}$ is the centerline value of the base velocity profile. The dimensional streamwise wavenumber in this initial profile is $\alpha = 1.12$ and $\beta = 2.1$ for the spanwise wavenumber. The Reynolds number is taken to be $\mathrm{Re} = \mathscr{U}\delta/\nu = 5000$, where ν is the kinematic viscosity. According to linear stability theory, the 2D TS and 3D oblique waves included in the initial condition are considered to be stable at this Reynolds number.

The flow is confined between two no-slip walls located at $y = 0$ and $y = 2\delta$, with periodic boundary conditions imposed in the homogeneous x and z directions. Domain extents are taken to be $[L_x, L_y, L_z]/\delta = [2\pi/\alpha, 2, 2\pi/\beta]$ and a constant mass flux condition is imposed. The flow configuration and initial condition is illustrated in Figure 1.

We consider the temporal evolution of this total flow field $\mathbf{u}_\mathrm{T}(x,y,z,t)$ in a RNL modeling paradigm. The RNL model consists of a streamwise-constant mean component, $\mathbf{U}(y,z,t) = \langle \mathbf{u}_\mathrm{T} \rangle_x$, which resolves the initial base profile $u_B(y)$, and a streamwise-varying perturbation component, $\mathbf{u}(x,y,z,t) = \mathbf{u}_\mathrm{T} - \mathbf{U}$ which resolves the 2D TS and 3D oblique waves, respectively $\mathbf{u}_{2D}$ and $\mathbf{u}_{3D}$ in equation (1). The angle brackets, $\langle\cdot\rangle_x$, denote the streamwise-averaging operation. A similar decomposition is assumed for the total pressure field, p_T. The RNL dynamics evolve according to the momentum equations,

$$\partial_t \mathbf{U} + \mathbf{U}\cdot\nabla\mathbf{U} + \rho^{-1}\nabla P - \nu\nabla^2\mathbf{U} = -\langle \mathbf{u}\cdot\nabla\mathbf{u}\rangle_x, \quad (2)$$

$$\partial_t \mathbf{u} + \mathbf{U}\cdot\nabla\mathbf{u} + \rho^{-1}\nabla p - \nu\nabla^2\mathbf{u} = -\mathbf{u}\cdot\nabla\mathbf{U}, \quad (3)$$

which are constrained to be divergence-free, $\nabla\cdot\mathbf{U} = \nabla\cdot\mathbf{u} = 0$, and ρ is the density. Including the nonlinear term, $\mathbf{u}\cdot\nabla\mathbf{u} - \langle\mathbf{u}\cdot\nabla\mathbf{u}\rangle_x$, in equation (3) recovers the Navier-Stokes equations. This term is omitted in the RNL equations to restrict perturbations interactions to those contributing to the mean dynamics.

The restriction placed on the perturbation dynamics restricts the streamwise-varying modes to those imposed in the equations and input through the initial perturbation assumed in equation (1), i.e., no modes become active through nonlinear interactions between perturbations. This restriction provides order-reduction and permits a tractable study of laminar-turbulent transition. The RNL model in this setting is equivalent to a simulation with only $N_x = 4$ grid points in the streamwise direction. We therefore also consider a simulation with $N_x = 6$ streamwise grid points in this study to allow energy to transfer to streamwise mode 2α. It should be emphasized that this simulation with $N_x = 6$ permits the streamwise wavenumber α to interact nonlinearly and give energy to this additional non-zero streamwise wavenumber; an interaction that is otherwise omitted in the RNL modeling paradigm.

We also consider truncating the number of spanwise modes included in these simulations to assess the potential for further order reduction. We consider simulations with $N_z = 6, 80, 160$ spanwise grid points, ranging from severe spanwise mode truncation to well-resolved. To assess model performance and accuracy, a DNS with $N_x = 160$ streamwise and $N_z = 160$ spanwise grid points is performed. Model predictions are compared to these DNS results throughout. The wall-normal grid is the same across all simulations and is stretched using a hyperbolic tangent function with $N_y = 192$ grid points.

The simulations are performed using a modified version of the pseudo-spectral LESGO code (https://lesgo.me.jhu.edu). Central finite differencing is used to evaluate wall-normal derivatives, and Fourier transforms are used for streamwise and spanwise derivatives. The 3/2-rule is used for de-aliasing. The fractional time-step method is used, with a Crank-Nicolson scheme for the wall-normal viscous terms and Adams-Bashforth for all other

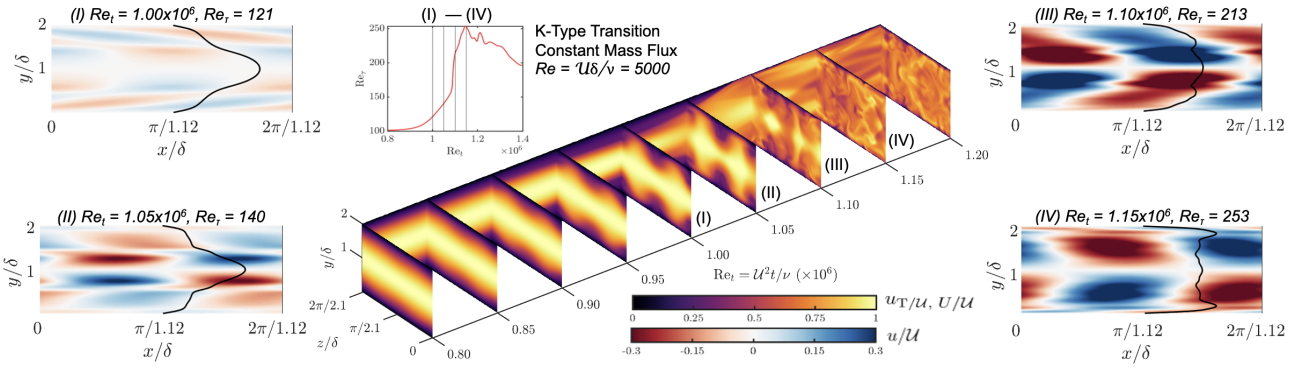

Figure 2. Evolution of RNL streamwise velocity. Center: Three-dimensional visualization of the streamwise component of the RNL mean velocity $U(y,z,t)$ at various points in time. The four surrounding contours show the streamwise component of the RNL perturbation field at mid-span at $\mathrm{Re}_t(\times 10^{-6}) = 1.00, 1.05, 1.10, 1.15$ with the mean component shown as a profile. A time history of the friction Reynolds number (center) is included for reference.

terms. The pressure Poisson equation is solved exactly by employing streamwise and spanwise Fourier transforms, discretizing the equation with finite difference and inverting the resulting tri-diagonal matrix.

RESULTS & DISCUSSION

We first discuss the evolution of the RNL dynamics through transition, which is illustrated in figure 2. A temporal Reynolds number, $\mathrm{Re}_t = \mathscr{U}^2 t/\nu$, is defined to distinguish different instances during this evolution. A time history of Re_τ is shown to capture the increase in friction velocity as the flow transitions to a turbulent state. The RNL dynamics are assessed by decomposing the flow field into streamwise-averaged mean and streamwise-varying perturbation components. Evolution of the streamwise component of the RNL mean velocity is shown as a 3D visualization (center). Four key instances at $\mathrm{Re}_t = 10^6, 1.05\times10^6, 1.10\times10^6, 1.15\times10^6$, respectively indicated by *(I)*, *(II)*, *(III)*, and *(IV)* are shown. The RNL perturbation component at mid-span at these instances are highlighted in the surrounding panels with the RNL mean velocity profile at this spanwise location superimposed.

The RNL perturbation component is shown to resolve Λ shapes near the wall. These perturbations interact nonlinearly to contribute to the RNL mean ($\langle \mathbf{u}\cdot\nabla\mathbf{u}\rangle_x$ in equation (2)). The mean component then forms a shear-layer at mid-span. Simultaneously, a streamwise-constant vortex-pair is formed. This vortex pair lifts-up low momentum fluid and leads to increased perturbation activity far from the wall. This behavior is clear at time instances *(I)* and *(II)*.The shear-layer that forms between near-wall Λ shapes and outer-layer fluid "roll up" across the single streamwise Fourier mode, redistributing momentum. The term "rolls up" is used loosely here as the true vorticity is approximated with a single streamwise mode. As momentum is redistributed, complex flow features develop and the near-wall velocity gradient increases (see *(III)* and *(IV)*).

The RNL transition mechanism described above is now compared to transition in DNS. Time histories of the friction Reynolds number for the temporally developing RNL simulation and a DNS are shown in figure 3(a). The RNL flow is shown to transition later than DNS data by an approximate time period of $\mathrm{Re}_t = 0.2\times10^6$. This delay is attributed to the omission of nonlinear interactions between streamwise-scales that saturate the TS wave but are not included the RNL dynamics. Despite this difference, the RNL model, with only one non-zero streamwise mode, is still able to transition to

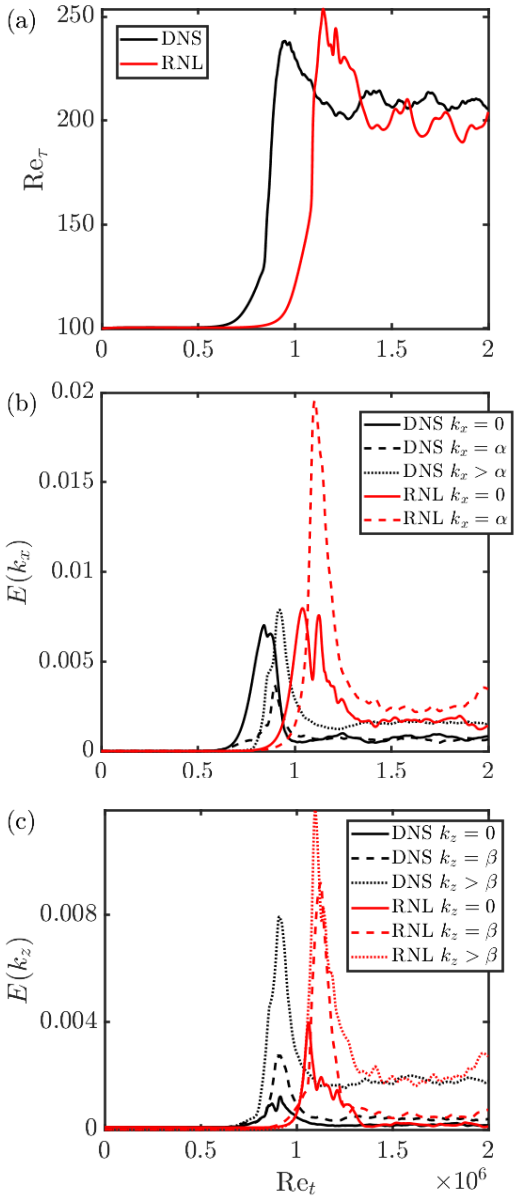

Figure 3. Time history of (a) wall-stress, and energy of (b) streamwise and (c) spanwise Fourier modes for DNS (black) and RNL (red). Dotted lines in (b) and (c) describe the total energy of all wavenumbers above the specified threshold.

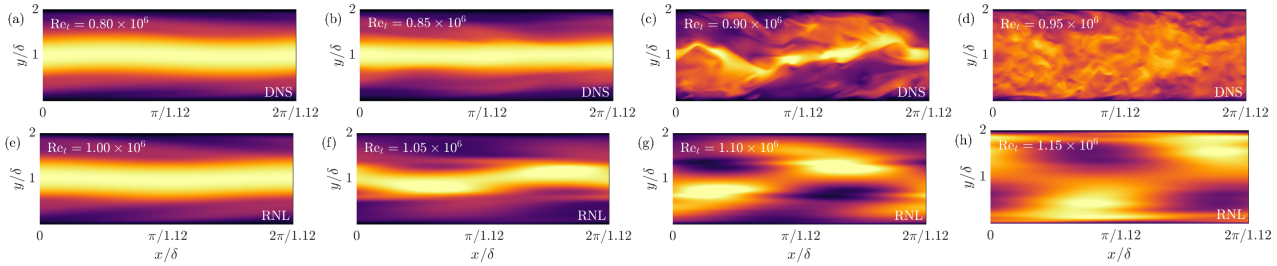

Figure 4. Streamwise component of the total velocity field for DNS (a-d) and RNL (e-h) at similar stages during their respective transition process. For RNL, the snapshots are taken at the times labeled I, II, II and IV in Figure 1. Corresponding DNS snapshots are taken at times $\mathrm{Re}_t(\times 10^{-6}) = 0.80, 0.85, 0.90, 0.95$, corresponding to similar stages of transition (which initiates at an earlier time in DNS versus RNL). The color limits are the same as those provided in Figure 1.

a turbulent state in a manner similar to DNS. Furthermore, once Λ shapes are present in the flow, the time it takes for RNL to transition to a turbulent state is similar to DNS. This indicates that streamwise-varying interactions primarily dictate when transition occurs; but once transition has begun, the process is predominantly driven by cross-stream interactions. LES models produced similar behavior, although the transition time was much closer to DNS with additional streamwise-varying modes available to support the LES dynamics (Schlatter *et al.*, 2004).

Another difference between the RNL model and DNS friction Reynolds number time evolution is the peak value. The RNL model achieves a higher wall-stress compared to DNS. To examine why this would be the case, we review time-histories of the volume-averaged energy of the streamwise and spanwise modes for DNS and the RNL model, respectively shown in figure 3(b,c). By omitting energy transfer to other streamwise-varying modes, the only streamwise-varying mode α in the RNL model achieves a higher energy state than DNS. This mode then transfers energy back to the streamwise-mean component resulting in a second peak and therefore results in a higher peak wall-stress compared to DNS. Spanwise modes are also shown to attain higher energy states to compensate for the lack of streamwise-scales resolved in the RNL model. This is consistent with previous work on the RNL model that has shown the RNL spanwise wavenumber support naturally adjusts energetics to accurately predict low-order statistics (Gayme & Minnick, 2019).

Figure 4 compares the total RNL and DNS streamwise velocity components at similar times during their respective transition processes. As expected, the flows are initially similar as the TS wave dominates. Once the shear layer begins to roll-up (visualized in panels c and g), additional streamwise modes become active in the DNS, whereas the single streamwise mode in the RNL dynamics continues to gain energy to compensate for the absent streamwise modes. Despite the lack of available energy exchange between streamwise Fourier modes in the RNL model, the single mode evolves towards a state comparable to a spatially filtered DNS during shear layer roll-up. In LES studies of this K-type transition, the sub-grid scale (SGS) model was shown to influence the evolution of transitional structures Schlatter *et al.* (2006). Given the similarities of the RNL model structures, we expect the form of these transitional structures is more dependent on spanwise grid resolution; a notion we now further explore.

We had previously found energy of spanwise modes plays an important role in the RNL transition process, potentially compensating for the omission of a range of streamwise modes and more specifically nonlinear interactions between them. To explore this role, we reduce the number of spanwise-modes supporting the RNL dynamics and study how this effects transition prediction. We consider two levels of truncation, mild with $N_z = 80$ and severe with $N_z = 6$. No LES like sub-grid scale model is considered to make up for the omission of smaller x and z scales. Time histories of the friction Reynolds number and energy of streamwise and spanwise modes are shown in figure 5 and compared to the RNL model with full spanwise support ($N_z = 160$). All cases considered in figure 5 consist of the same single non-zero streamwise wavenumber ($k_x = \alpha$) that is initially active from the initial condition.

Spanwise-mode truncation has little effect on transition timing. Even the severe truncation case predicts transition near the same time as the RNL model, albeit a little earlier. Additionally, all cases with $N_x = 4$ (i.e., one nonzero streamwise mode $k_x = \alpha$) are shown to predict a similar peak friction Reynolds number. Although there are fewer spanwise modes, the near-wall Λ structures remain sufficiently resolved during the earlier stages of transition. As a result, the streamwise vortex pair develops in a similar amount of time to the well-resolved RNL simulation. This suggests the limited number of spanwise modes can resolve the shear-layer roll-up process.

We now consider time histories of the streamwise and spanwise mode energy that is also shown in figure 5. The evolution of the streamwise-mean and single non-zero streamwise mode energy remain relatively similar among all cases. This suggests the energetics of these streamwise wavenumbers is mostly supported by lower spanwise wavenumbers and not the higher wavenumbers that have been omitted. Notable variability is however observed among the spanwise mode energetics. The case with severe spanwise mode truncation is shown to have higher mean spanwise energy and consequently lower energy for spanwise wavenumbers greater than β, where for the case with $N_z = 6$, there is only one spanwise wavenumber greater than β included. Similar to previous findings, this behavior is attributed to the reduced dynamics naturally adjusting for the lack of spanwise wavenumber support.

We now attempt to augment the RNL model to improve transition time prediction. As discussed previously, the delayed transition was attributed to the RNL model's inability to saturate the TS wave without additional streamwise-varying modes. We therefore consider including an additional streamwise-varying mode, 2α. For an additional streamwise-varying mode to become active given the initial condition considered here, nonlinear interactions between streamwise-varying modes must be included in the dynamics. Here, we introduce this additional streamwise-varying mode by simply taking $N_x = 6$. In this manner, the mode α may self-interact to contribute to mode 2α. This greatly increases model complex-

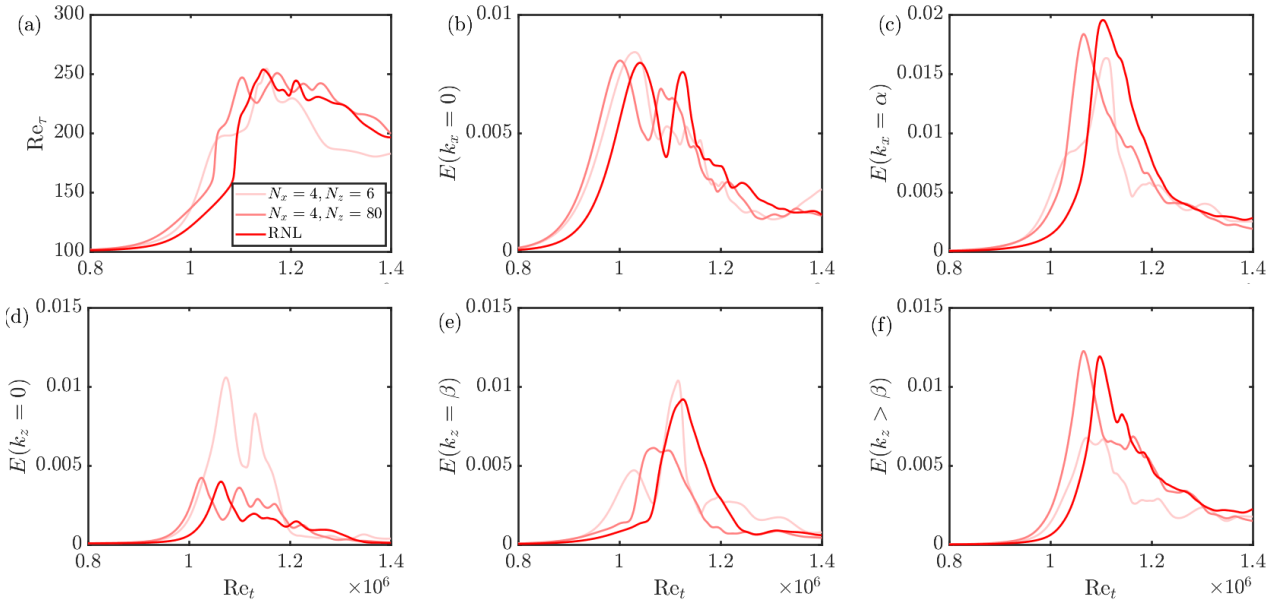

Figure 5. (a) Wall-stress for the RNL model ($N_x=4, N_z=160$) with mild ($N_x=4, N_z=80$) and severe ($N_x=4, N_z=6$) spanwise mode truncation. Energy of the (b) streamwise mean ($k_x=0$), (c) single non-zero streamwise Fourier mode ($k_x=\alpha$), (d) spanwise mean ($k_z=0$), and (e) spanwise Fourier mode ($k_z=\beta$) for these simulations is also shown. Panel (f) shows the cumulative energy of spanwise Fourier modes greater than β. Note the time-period shown is shortened to highlight key features of the transition process.

ity and the amount of nonlinear interactions; from a system with a single non-zero wave number permitting only nonlinear interactions that produce $k_x=0$ to the full range of interactions for 3 streamwise Fourier modes. However, we still consider this model with $N_x=6$ to be tractable.

Time histories of the friction Reynolds number and streamwise/spanwise mode energy is shown in figure 6 for DNS and cases with $N_x=6$. With the addition of another streamwise-varying mode, we note a significant improvement in transition prediction compared to DNS. By allowing the TS wave to transfer energy to another streamwise-varying mode that is not initially active, there is sufficient enough TS wave saturation to transition the flow from a laminar state at an earlier time. Furthermore, the transition time is predicted to be slightly sooner than DNS. It is worth noting that the friction Reynolds number peak is still over-predicted compared to DNS. Furthermore, the predicted transition time for these simulations with $N_x=6$ is comparable to LES studies with $N_x=32$ (Schlatter *et al.*, 2004), suggesting additional streamwise mode interactions are not needed to capture when the flow transitions to a turbulent state.

When comparing the time histories of the streamwise mode energies, we note that the streamwise-mean energy is comparable to DNS. Similar to the RNL model, the energy of mode α is higher than DNS due to the streamwise mode truncation. The energy of the additional mode 2α, however, is similar to the composed energy of all other modes in the DNS. This highlights the success of predicting transition for this flow with only $N_x=6$ grid points; the transition process is predominantly driven by the evolution of the TS wave. Also, similar to the RNL model, the energy of the spanwise modes is shown to be higher than DNS, this once again is attributed to spanwise wavenumber support modification that naturally occurs for reduced streamwise dynamics.

We now impose spanwise mode truncation for the simulation with $N_x=6$. Time histories with mild ($N_z=80$) and severe ($N_z=6$) spanwise mode truncation are included in figure 6. The case with mild spanwise mode truncation is shown to transition earlier, and coincidentally the case with severe truncation, $N_z=6$, transitions at the same time as the DNS. The energy of the streamwise modes for these cases remains similar to the case with full spanwise-grid resolution, $N_z=160$, although the streamwise-mean energy for the severe truncation case is smaller. Conversely the spanwise-mean energy for this severe truncation case is higher, as the spanwise wavenumber represented by the oblique wave.

CONCLUSION

RNL simulations of temporal K-type transition revealed key nonlinear interactions between the streamwise-averaged mean and streamwise-varying perturbations. RNL dynamics supported by a single streamwise-varying Fourier mode, initially excited by a 2D TS wave and 3D oblique wave, interacting with the streamwise mean, captures prominent flow features such as Λ-shaped structures and a streamwise vortex pair. A comparison to DNS indicated that streamwise-varying interactions primarily dictate when transition occurs; however, once transition has begun, the process is predominantly driven by cross-stream interactions. Additionally, the RNL dynamics were shown to naturally compensate for the absence of streamwise-varying modes by achieving a higher energy state in the spanwise wavenumbers supporting the dynamics.

These findings motivated additional reduced-order model simulations where the spanwise wavenumber support was truncated and a model with two streamwise-varying modes were permitted to interact nonlinearly. It was shown that reducing the number of spanwise modes did not significantly modify the timing of laminar-turbulent transition, however an additional streamwise-varying mode allowed to nonlinearly interact with the TS wave mode greatly improved this timing compared to DNS. This work shows the RNL framework is capable of not only resolving key transitional flow structures, but also has the potential to act as the foundation for a minimal model for transition.

Various future avenues may be pursued to develop a min-

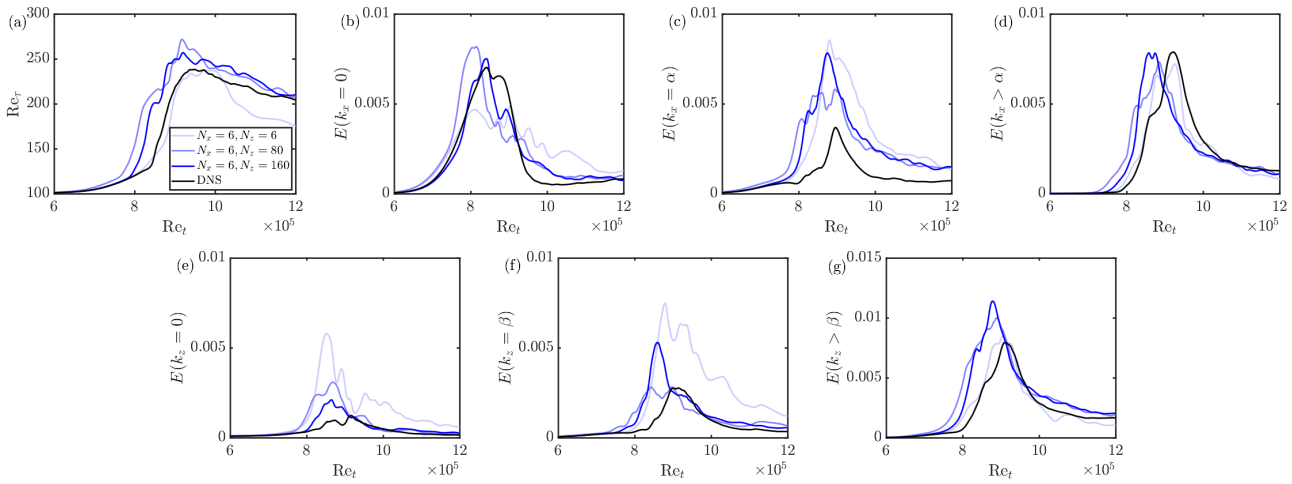

Figure 6. (a) Wall-stress for simulations with $N_x = 6$ and varying levels of spanwise mode truncation compared to DNS (black). Energy of the (b) streamwise mean ($k_x = 0$), (c) single non-zero streamwise Fourier mode ($k_x = \alpha$), (e) spanwise mean ($k_z = 0$), and (f) spanwise Fourier mode ($k_z = \beta$) for these simulations is also shown. Panel (d) shows the energy of streamwise Fourier mode $k_x = 2\alpha$, compared to the cumulative energy of streamwise mode 2α and greater simulated in DNS. Panel (g) shows the cumulative energy of spanwise Fourier modes greater than β. Note the time-period shown is shortened to highlight key features of the transition process.

imal transition model. First, the methodology presented here should be extended to study other modes of transition, e.g. H-type, with streamwise and spanwise wavenumber supports corresponding to the specific initial condition considered. This could then aid the development of a minimal transition model for WMLES, where only the dynamics of required modes are simulated near the wall. This effort could be further aided by incorporating methods from studies of parabolized stability equations.

FUNDING ACKNOWLEDGMENT

This work was supported by the In-house Laboratory Independent Research (ILIR) program, Problem Element 0601153N, managed by the NSWC Carderock Division Office of Technology and Innovation for the Office of Naval Research. Computations employed Advanced Research Computing at Hopkins core facility (rockfish.jhu.edu), which is supported by the National Science Foundation (OAC1920103).

REFERENCES

Aram, S., Shan, H., Jiang, L. & Atsavapranee, P. 2022 *Numerical Analysis of Natural Boundary Layer Transition and Trip Effect on Inclined Spheroid*.

Gayme, D. F. & Minnick, B. A. 2019 Coherent structure-based approach to modeling wall turbulence. *Phys. Rev. Fluids* **4**, 110505.

Han, B.Z., Huang, W.X. & Xu, C.X. 2024 A combined active control method of restricted nonlinear model and machine learning technology for drag reduction in turbulent channel flow. *J. Fluid Mech.* **993**, A4.

Jung, Y. & Baeder, J. 2023 Uncertainty quantification of laminar–turbulent transition on airfoil and fuselage. *J. Aircraft* **60** (6), 1746–1760.

Klebanoff, P. S., Tidstrom, K. D. & Sargent, L. M. 1962 The three-dimensional nature of boundary-layer instability. *J. Fluid Mech.* **12** (1), 1–34.

Lee, C.B. & Jiang, X.Y. 2026 *Flow Structures in Transitional and Turbulent Boundary Layers*, pp. 85–142. Singapore: Springer Nature Singapore.

Lozano-Durán A., Hack M. J. P. & Moin, P. 2018 Modeling boundary-layer transition in direct and large-eddy simulation using parabolized stability equations. *Phys. Rev. Fluids* **3**, 023901.

Marxen, O. & Zaki, T. A 2019 Turbulence in intermittent transitional boundary layers and in turbulence spots. *J. Fluid Mech.* **860**, 350–383.

Menter, F, Matyushenko, A., Lechner, R., Stabnikov, A. & Garbaruk, A. 2022 An algebraic lctm model for laminar–turbulent transition prediction. *Flow, Turb. & Comb.* **109**.

Minnick, B. A. & Gayme, D. F. 2024 Restricted nonlinear boundary layers over a moving wall. In *Int'l Symposium on Turb. and Shear Flow Phenomena (TSFP-13)*.

Narasimhan, G., Meneveau, C. & Zaki, T. A. 2021 Large eddy simulation of transitional channel flow using a machine learning classifier to distinguish laminar and turbulent regions. *Phys. Rev. Fluids* **6**, 074608.

Risha, A. C., Minnick, B. A. & Gayme, D. F. 2026 Restricted nonlinear investigation of developing boundary layers over decelerating walls. *J. Physics: Conference Series* **3173** (1), 012015.

Schlatter, P., Stolz, S. & Kleiser, L. 2004 Les of transitional flows using the approximate deconvolution model. *Int'l J. Heat and Fluid Flow* **25** (3), 549–558, turbulence and Shear Flow Phenomena (TSFP-3).

Schlatter, P., Stolz, S. & Kleiser, L. 2006 Applicability of les models for prediction of transitional flowstructures. In *IUTAM Symposium on Laminar-Turbulent Transition* (ed. Rama Govindarajan), pp. 323–328. Dordrecht: Springer Netherlands.

Thomas, V., Farrell, B., Ioannou, P. & Gayme, D. F 2015 A minimal model of self-sustaining turbulence. *Phys. Fluids* **27**, 105104.

Y. Mori, A. Yakeno & Obayashi, S. 2024 Coherent wave generation in swept-wing boundary layer transition at a real flight condition. In *Int'l Symposium on Turb. and Shear Flow Phenomena (TSFP-13)*.

Zaki, T. A. 2013 From streaks to spots and on to turbulence: Exploring the dynamics of boundary layer transition. *Flow, Turb. & Comb.* **91** (3), 451–473.